# Assessment of microcapsule—catalyst particles healing system in high performance fibre reinforced polymer composite

P A Bolimowski[1,2], D F Wass[1] and I P Bond[2]

[1] School of Chemistry, University of Bristol, Cantock's Close, BS8 1TS Bristol, UK

[2] Advanced Composites Centre for Innovation and Science (ACCIS), University of Bristol, Queen's Building, University Walk, BS8 1TR Bristol, UK

E-mail:
patryk.jarzynka@bristol.ac.uk, duncan.wass@bristol.ac.uk and i.p.bond@bristol.ac.uk

Abstract

Autonomous self-healing in carbon fibre reinforced polymer (CFRP) is demonstrated using epoxy resin filled microcapsules and a solid-state catalyst. Microcapsules filled with oligomeric epoxy resin (20–450 μm) and particles of $Sc(OTf)_3$ are embedded in an interleave region of a unidirectional CFRP laminate and tested under mode I loading. Double cantilever beam (DCB) test specimens containing variable concentrations of microcapsules and catalyst were prepared, tested and compared to those healed by manual injection with corresponding healing resin formulation. The healing efficiency was evaluated by comparing the maximum peak load recorded on load–displacement curves for pristine and healed specimens. A 44% maximum recovery was observed for specimens containing 10 wt% of solid phase catalyst and 11 wt% of epoxy microcapsules. However, a significant (80%) decrease in initial strain energy release rate ($G_{IC}$) was observed for specimens with the embedded healing chemistries.

Keywords: self-healing, CFRP, epoxy microcapsules, catalyst, mode I interlaminar fracture toughness

## 1. Introduction

Fibre reinforced polymer (FRP) composites are increasingly used in industries like aerospace, energy, automotive and in offshore structures due to their exceptional specific mechanical properties compared to conventional materials [1]. In service, FRPs are susceptible to internal damage, including matrix cracking, fibres fracture, and delamination between plies. When undetected and unrepaired, these damages can be of significant detriment to performance, ultimately leading to premature failure. It can be addressed by embedding func-tionality capable of effecting autonomous repair, minimising often complicated and difficult damage detection strategies and manual maintenance [2–4].

Self-healing has already been widely studied in polymers and the fibre reinforced composites where autonomous repair has been achieved through a range of approaches [2–4] including embedding healing-agent-filled microcapsules [5–23], hollow fibres [24–26] or incorporating vascular networks capable of delivering various healing chemistries [27, 28]. These systems are considered as extrinsic, and mean that the healing chemistries are introduced externally into the crack planes. Another approach described in the literature includes intrinsic mechanisms, where the polymer is capable of healing without any external supply of healing agent [29–34]. The most developed approach to date sees microencapsulation of a healing monomer or oligomer within a polymeric shell, which are then embedded in a host material. Embedded

microcapsules are ruptured by a propagating crack to release the healing agent, upon subsequent chemical reaction or physicochemical processes, new polymer bonds the fracture surfaces and restores the lost material properties [2–4].

The first and most widely exploited microencapsulation system was proposed in 2001 by White et al [5]. In this approach, microencapsulated dicyclopentadiene (DCPD) was embedded in an epoxy polymer and polymerised following release in the presence of ruthenium Grubbs' catalyst (ring opening metathesis polymerisation—ROMP). Despite high healing efficiencies [3], the high price of the ruthenium cat-alyst and its low stability in the presence of moisture, amine hardeners and oxygen, limited its commercialisation. Several modifications were proposed including protecting the Grubbs' catalyst in wax or usage of alternative second generation, Hoveyda–Grubbs' and Tungsten hexachloride as catalysts [6–8]. However, these barriers still limit DCPD/Grubbs' system wider application in autonomous healing materials. To over-come some of these issues and to provide a healing system that is chemically and mechanically compatible with a typical host epoxy matrix, less expensive diglycidyl ether of bisphenol A (DGEBA) was demonstrated as an alternative healing agent [7–14]. Encapsulated DGEBA was combined with a variety of hardeners, including catalytic curing agents [9, 10, 20] and multifunctional amines [11–14]. In the most recent work, Coope et al [9] utilised scandium (III) triflate particles as a catalytic curing agent for an epoxy resin. A maximum of 80% of healing efficiency was achieved at ele-vated temperatures using tapered double cantilever beam (DCB) test specimens in a low temperature curing epoxy [9]. In other approaches, liquid phase and relatively toxic curing agents were utilised, such as boron trifluoride etherate hard-ener ($(C_2H_5)_2O \cdot BF_3$) [10], epoxy/mercaptan [11, 12] and epoxy/amine chemistry [13, 14]. Within these works, two types of capsules were utilised to successfully separate the healing chemistries from the surrounding environment and the healing efficiency was often dependent on stoichiometric ratio and contact of both healing components.

An alternative, single capsule approach to self-healing was demonstrated in the literature and utilised the inherent residual functionality of the host epoxy [2–4]. Healing is achieved via interaction of encapsulated solvent with residual functionality in the epoxy polymer. For instance, almost full recovery of mode I fracture toughness was demonstrated using solvent (ethyl phenylacetate) filled microcapsules [15, 16, 23]. Non-fully cured epoxy matrix is swollen by the solvent released from microcapsules and the residual func-tional groups initiate further crosslinking which re-bond fractured surfaces. The system was modified by use of shape memory alloys (SMA) to reduce the separation after fracture damage and to enhance the healing performance [17, 18]. However, the need for unreacted functional groups in under-cured epoxy limits the broader applications of this self-heal-ing system. Other, latent functionality was also proposed by Yin et al [19] where hardener dispersed in the matrix ($CuBr_2$(2-methylimidazole)$_4$) was available for a healing reaction, but required heating to 130 °C to polymerise the released resin. Moreover, Xiao et al [20] studied a system using the $(C_2H_5)_2O \cdot BF_3$ catalyst absorbed by short sisal fibres and protected by a polystyrene coating.

In this work we demonstrate an autonomous self-healing unidirectional fibre reinforced composite structure of com-mercially available epoxy resin/carbon fibre resin tape (SE 70, Gurit, UK). Self-healing was achieved by embedding of epoxy resin filled microcapsules (20–450 μm) and solid state catalyst ($Sc(OTf)_3$) in a damage region. The main aim of this work is optimisation and assessment of the selected system as a self-healing function within a high performance composite structure. Microencapsulated self-healing has already been demonstrated in epoxy polymers and their composites with woven fibres, however, application in unidirectional compo-sites is relatively unexplored. A maximum mode I DCB recovery of 42% is achieved for an autonomous system which is comparable to a manually initiated approach (52%). However, the high healing efficiency is associated with sig-nificant detrimental effect on the host polymer fracture properties. Nevertheless, it is demonstrated that micro-encapsulated self-healing can be achieved in a unidirectional composite cured at high temperature (100 °C) using a microcapsule—catalyst approach and that the healing func-tionality can be optimised to avoid any significant detrimental effects.

In general, the selected epoxy resin–organic solvent system was encapsulated in a poly(urea-formaldehyde) shell using a standard processing technique described in the lit-erature [21]. Microcapsules and commercially sourced cata-lytic curing agent were embedded in an interleave region of a FRP laminate using standard hand lay-up techniques. After initial DCB tests to assess mode I strain energy release rate ($G_{IC}$) recovery, the volume of embedded epoxy resin and catalyst loading were varied in order to assess the healing rate. Herein the effect of both components on the damage region is demonstrated and discussed in detail. Microcapsules con-taining DGEBA (75 wt%) and high boiling point organic solvent, ethyl phenylacetate (25 wt%) have been documented in previous studies as an effective application of self-healing epoxides [9]. Scandium (III) triflate ($Sc(OTf)_3$) was selected as a suitable initiator due to its stability and catalytic activity in the polymerisation of epoxy resins [9, 35–37]. Further-more, $Sc(OTf)_3$ embedded in a carbon fibre reinforced poly-mer (CFRP) composite has been demonstrated as being capable of repeated healing via microvascular channels [37].

## 2. Materials and methods

### 2.1. Materials

Ethyl phenylacetate (EPA, $C_6H_5CH_2C(O)OC_2H_5$), urea ($NH_2CONH_2$), poly(ethylene-alt-maleic anhydride) (EMA, $M_w$ = 100 000–500 000, powder); resorcinol ($C_6H_4$-1,3-$(OH)_2$), formaldehyde (37 wt% in $H_2O$), ammonium chloride ($NH_4Cl$) and scandium (III) triflate ($Sc(OTf)_3$) were pur-chased from Sigma-Aldrich and used as received. Sodium hydroxide (NaOH) was purchased from Fisher Scientific. Commercial epoxy resin—EPON 828 was purchased from

Table 1. Designation of all tested DCB specimens and composition of interleaf resin present in the damage region.

| Specimen type | Healing mechanism | Microcapsules size | Epoxy microcapsules (wt%)[a] | Catalyst load (wt%)[a] |
|---|---|---|---|---|
| Control 1 | Manual | — | — | — |
| Control 2 | — | — | — | — |
| Autonomous | | 20–450 | 26 | 2.5 |
| 5.5 wt_2.5 wt% | | | 5.5 | 2.5 |
| 11 wt_2.5 wt% | | | 11 | 2.5 |
| 26 wt_2.5 wt% | | | 26 | 2.5 |
| 11 wt_0.0 wt% | Autonomous | 250–450 | 11 | 0 |
| 11 wt_1.0 wt% | | | 11 | 1.0 |
| 11 wt_5.0 wt% | | | 11 | 5.0 |
| 11 wt_10 wt% | | | 11 | 10 |

[a] Microcapsules and catalyst weight loading calculated relatively to SA 70 epoxy resin used as the filler.

PolySciences, Inc. Carbon fibre/epoxy resin tape (SE 70) and adhesive resin film (SA 70) were sourced from Gurit, UK and also used as received.

## 2.2. Methods

2.2.1. Microencapsulation. Microcapsules containing epoxy resin and organic solvent were prepared by in situ polymerisation in an oil-in-water emulsion [21]. Briefly, 60 ml of water phase containing 1 wt% of emulsion stabiliser (EMA) was prepared in a round bottomed vessel and subsequently 1.25 g of urea, 0.125 g of resorcinol and 0.125 g of ammonium chloride were added and dissolved. After that, the pH of the water phase was adjusted by dropwise addition of NaOH (≈0.2 N) to 3.10. Stirring speed was increased to 800 rpm and 30 ml of measured oil phase was added dropwise. 3.16 g of formalin was added and the temperature was increased to 55 °C. After 4 h, the stirrer was stopped, and the microcapsule slurry was left in the water medium for 24 h at ambient temperature. Next, microcapsules were filtered in order to separate capsules with desired size. Capsules were vacuum filtered and rinsed a few times with ethanol/water. The isolated capsules were post heated at 55 °C in an oven for 2 days. Yield of microcapsules was calculated relative to mass of used materials (Y%).

2.2.2. Microcapsule analysis. Microcapsule diameter and size distribution was analysed by a Zeiss optical microscope AX10, Imager.M2 equipped with a video camera AxioCam. ICc 1. For the size distribution, image analysis software (ImageJ) was used. Mean diameter and size distribution were obtained from at least 500 measurements of capsule diameter. Surface morphology analysis for dry microcapsules was performed with a scanning electron microscope JOEL SEM 5600LV. Thermal stability of microcapsules was determined using thermogravimetric analysis (TGA). Mass loss of microcapsules was recorded during non-isotherm from 25 °C to 500 °C and isothermal measurements at using a TA Instruments Q500 TGA.

2.2.3. Composite manufacturing. Composites with embedded healing chemistries were manufactured using unidirectional carbon/epoxy resin tape (SE 70, Gurit UK) and adhesive resin film (SA 70, Gurit, UK) by standard hand-lay up technique (16 plies—160 mm × 195 mm). Laminates after lay-up were vacuum bagged on an aluminium tool plate and consolidated according to the manufacturer's recommendations (at 100 °C for 100 min) under vacuum of 660–710 mmHg. The artificially created damage region was filled with a resin paste (SA70 resin film) containing healing chemistries at the desired weight loading (table 1). The filling paste was prepared by dispersion of dry capsules and/or catalyst at 65 °C. Each panel was equipped with a release film at 85 mm from the edge of specimens overlapping at minimum 500 μm of the resin pocket. The detailed configuration of the system is presented in the figure 1. After curing, composite plates were removed from the vacuum bag and a 30 mm region from the panel front was grit blasted. Composite plates were then trimmed and cut into DCB specimens (20 mm × 175 mm). Piano hinges were bonded to the specimens at the pre-cracked end using Araldite 2014 structural adhesive and left at ambient temperature until fully cured.

2.2.4. Types of specimens and geometry. The DCB tests specimens were used to quantify mode I recovery using manual and autonomous approaches to self-healing. The specimen geometry was adapted from the ASTM standard test method 5528-01 [38].

Two types of control specimens were manufactured and tested in order to determine a benchmark of the composite fracture properties and the effect of embedded SA 70 (Gurit, UK) resin interleaf. The Control 1 specimens, containing no additional interleaves, was used to determine the fracture properties of selected composite material (SE 70, Gurit, UK) and to determine a benchmark for mode I recovery using the resin formulation described in the literature [37]. Specimens were fractured according to the standard test method [38] and manually injected with liquid resin—catalyst formulation. After self-healing processes, the specimens were retested using the same approach. The Control 2 (figure 1) was used to determine the virgin fracture properties of the modified DCB geometry. This geometry was used in order to control the propagating crack from the non-bonding insert to the end of

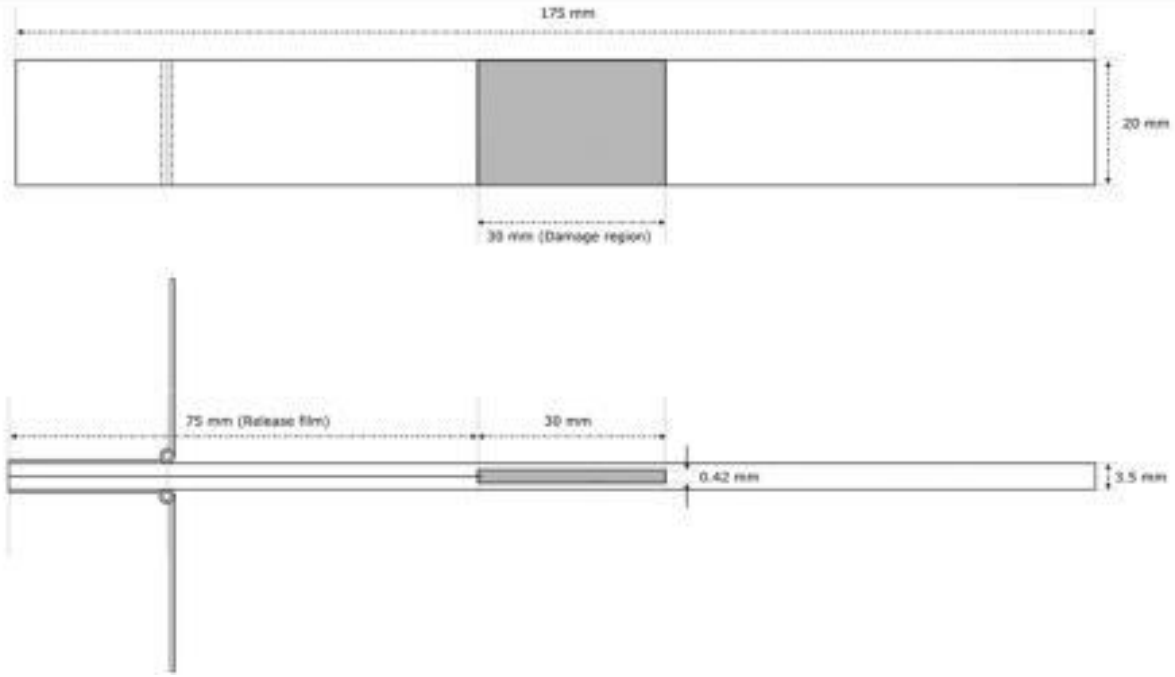


Figure 1. CFRP double cantilever beam specimen (DCB) geometry adopted from ASTM standard test method 5528-01 [38], containing artificially created damage region with embedded self-healing chemistries.

resin pocket through the embedded microcapsules and catalyst particles. Subsequently, the epoxy microcapsules and catalyst particles were embedded in the interleaf at various combinations. The crack introduced during mode I DCB testing ruptures microcapsules causing release of liquid monomer and subsequent contact with embedded particles of $Sc(OTf)_3$. The detailed test specimen's configurations are summarised in table 1. First, specimens containing literature loadings of microcapsules and the catalyst [9] were tested as the proof of concept for autonomic self-healing. The effect of microcapsules loading was determined at constant concentra-tion of the catalyst (2.5 wt%) and from 5.5 to 26 wt% of microcapsules. The effect of $Sc(OTf)_3$ particles was deter-mined later at constant loading of microcapsules (11 wt%) and variable concentration of the catalyst ranging from 1 to 10 wt%. It should be noted here that the weight fraction of the catalyst and microcapsules was measured relatively to the resin used as filler in the resin pocket.

2.2.5. Mode I DCB fracture toughness (strain energy release rate) tests and healing quantification. An electromechanical test machine (Shimadzu AGX-X) equipped with 1 kN load cell and a video camera was used in opening mode I interlaminar fracture tests for virgin and healed DCB tests specimens. Tests were performed in accordance to the ASTM 5528-01 standard method [38]. Specimens were tested in crack opening mode at 3 mm $min^{-1}$ displacement rate, from the release film to the end of interleave resin region containing microcapsules. After testing, specimens were unloaded, sealed and left at 80 °C for 24 h. Healed specimens were retested using the same methodology.

The healing efficiency ($\eta$) was calculated from the ratio of the healed maximum peak load ($P_{Healed}$) to the virgin maximum peak load ($P_{Virgin}$)

$$h = \frac{P_{\text{Healed}}}{P_{\text{Virgin}}} \cdot 100\%.$$

Values of initial opening mode I interlaminar strain energy release rate ($G_{Ic}$) were determined for various specimens to demonstrate the effect of healing chemistries on the composite. The $G_{Ic}$ values were calculated at the point of deviation from linearity on the load–displacement curves:

$$G_{Ic} = \frac{3Pd}{},$$

where P is the applied load at the onset of nonlinearity, $\delta$ is the load point displacement, b and a are specimen average width and delamination length respectively.

## 3. Results

### 3.1. Microencapsulation

Microcapsules containing the DGEBA were synthesised using in situ polymerisation in an oil-in-water emulsion [39]. Size distribution, corresponding scanning electron micro-graphs and results for thermal stability are presented in figure 2.

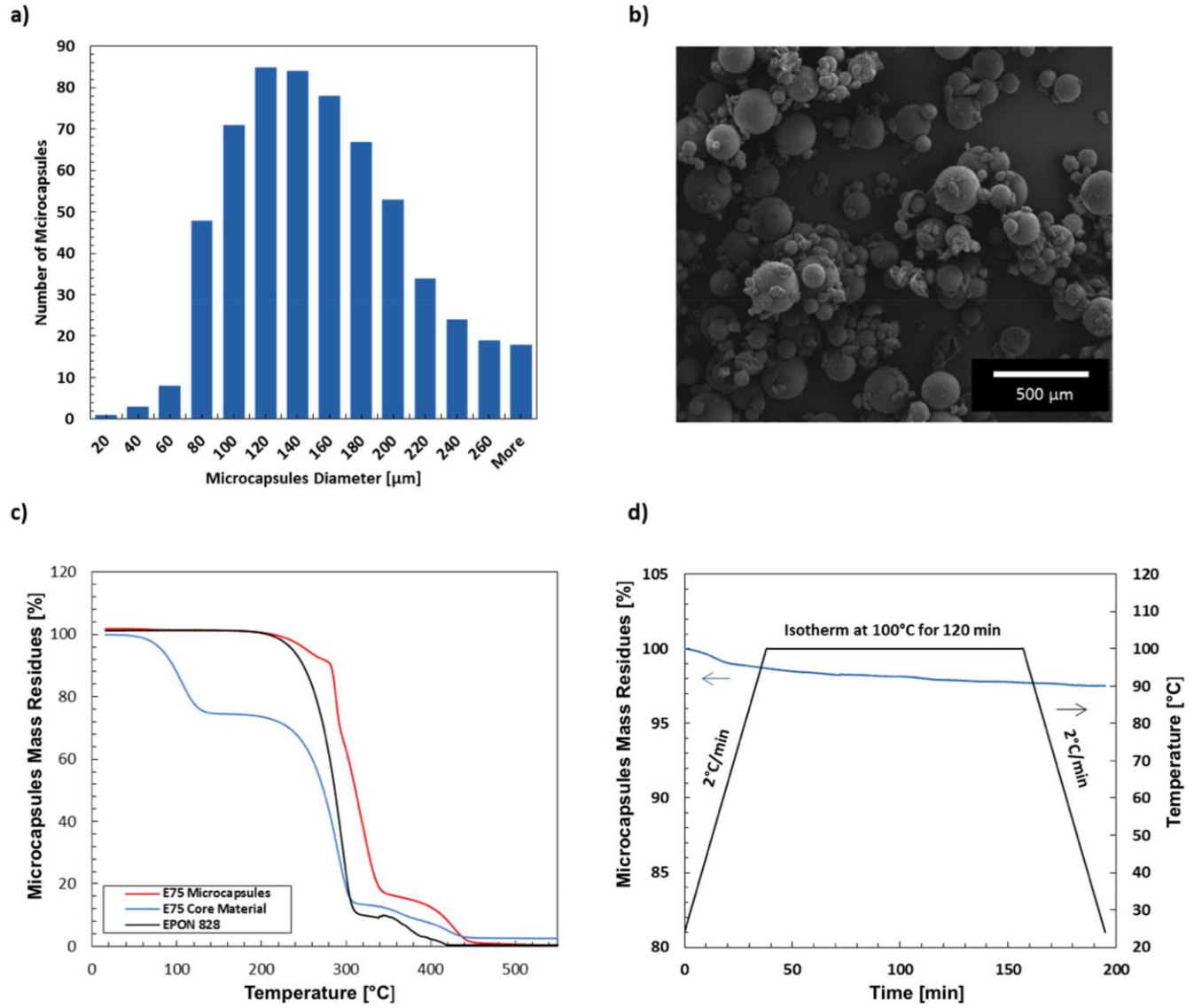


Figure 2. (a) Size distribution of prepared poly(urea-formaldehyde) microcapsules containing 75 wt% of epoxy resin (EPON 828) and 25 wt% of organic solvent (ethyl phenylacetate—EPA); (b) corresponding SEM image; (c) representative non-isothermal and (d) isothermal TGA traces for the microcapsules.

Microcapsules after synthesis exhibited a wide size distribution ranging from 20 to 420 µm in diameter (figure 2(a)). The microencapsulation efficiency calculated according to the mass of used chemicals in the process resulted in satisfactory 77%. Enclosed scanning electron micrograph (figure 2(b)) illustrate that the microcapsules have regular spherical shape and the shell wall is covered with rough polymeric layer of poly(urea-formaldehyde) [39]. The thermal stability of microcapsules was determined using TGA. The results of non-isothermal analysis indicated that microcapsules are stable to 170 °C (figure 2(c)). The first observed mass loss is associated with evaporation of ethyl phenylacetate (B.P. 229 °C) released from microcapsules. When poly(urea-for-maldehyde) decomposes, the organic solvent and epoxy resin are released and the organic solvent evaporates immediately. Increasing further temperature, a mass loss associated with the decomposition of DGEBA resin is observed. When the epoxy resin–organic solvent mixture is unprotected in polymeric shell, the increase of temperature and continues flow of purge gas (nitrogen), cause evaporation of the ethyl pheny-lacetate at much lower temperature. It is calculated that the solvent content in the healing resin is 25.4% and the epoxy resin is 74.6%. In addition, analysing figure 2(d) it is con-cluded that epoxy microcapsules are thermally stable when exposed to curing conditions of the selected carbon fibre/ epoxy resin pre-preg material (SE70 carbon/epoxy). A minor 2.5% mass loss calculated from the graph corresponds to water evaporation from the polymeric shell.

### 3.2. Manual healing

Blank DCB specimens were tested in order to determine a benchmark of mode I fracture toughness and self-healing using the resin formulation described in the literature as the most promising for such application [9, 36, 37]. After the

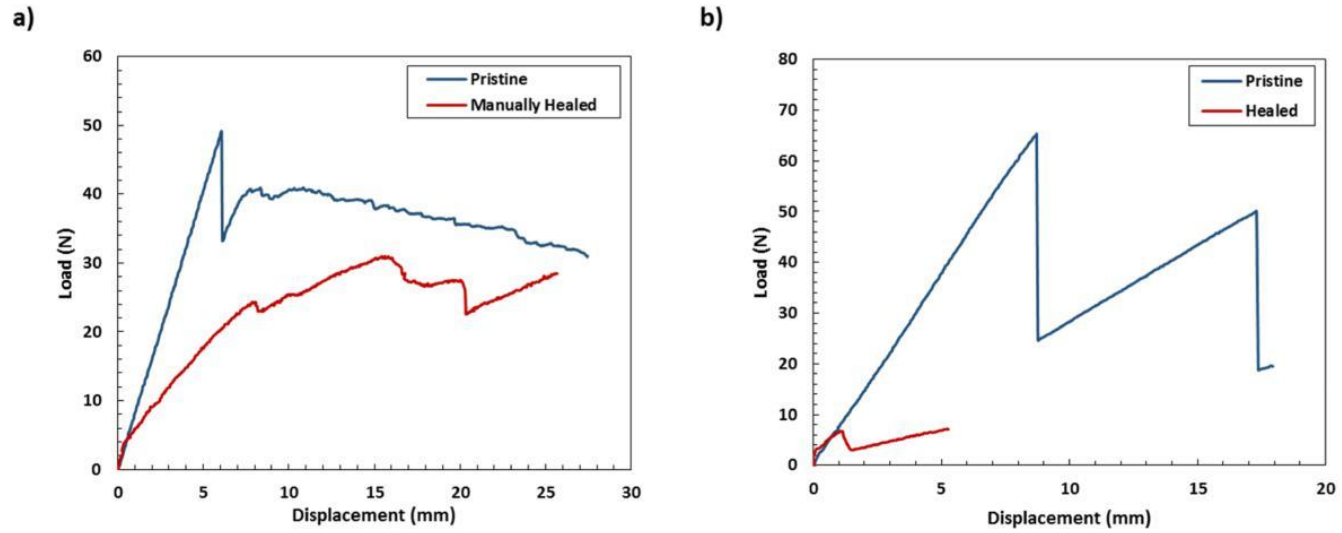


Figure 3. Typical load–displacement curves for virgin and healed (a) control specimens type 1 containing no interleave resin and (b) specimens containing 26 wt% of microcapsules and 2.5 wt% solid phase catalyst in the interleave.

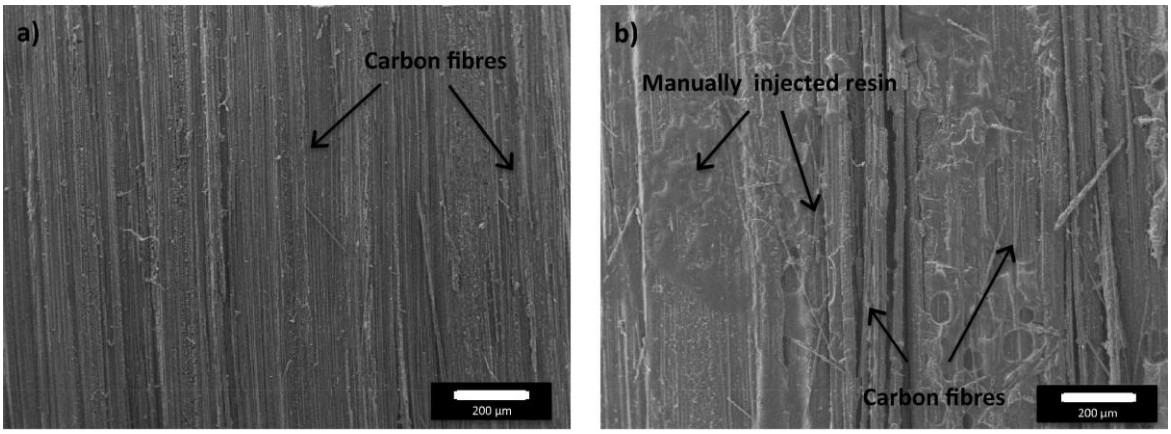


Figure 4. Fracture surfaces for control specimens type 1 (a) after initial fracture tests and (b) after manual repair and retest.

Table 2. Summary of healing efficiency (η) and initial fracture toughness ($G_{IC}$) in dependence on SH agent load/volume in the damage region.

| Designation | Vol % | Capsules size (µm) | Initial load $P_{Virgin}$ (N) | Healed load $P_{Healed}$ (N) | η (%) | Initial $G_{IC}$ (J m$^{-2}$) | Temp |
|---|---|---|---|---|---|---|---|
| Manual | — | — | 47.0 ± 1.3 | 24.7 ± 4.3 | 52.5 ± 8.9 | 413 ± 19 | |
| Autonomous | 26 | 20–450 | 57.2 ± 10.6 | 5.5 ± 1.5 | 9.9 ± 3.5 | 746 ± 97 | |
| Control 2 | — | — | 81.0 ± 6.4 | — | — | 1371 ± 224 | 80 °C |
| 5.5 wt_2.5 wt% | 5.5 | 250–420 | 71.0 ± 4.3 | 7.8 ± 2.0 | 10.7 ± 2.0 | 1076 ± 161 | |
| 11 wt_2.5 wt% | 11 | 250–420 | 77.0 ± 9.1 | 8.6 ± 1.8 | 11.3 ± 3.3 | 1311 ± 326 | |
| 26 wt_2.5 wt% | 26 | 250–420 | 68.4 ± 3.5 | 6.8 ± 1.7 | 11.8 ± 2.5 | 997 ± 86 | |

initial fracture tests, the DCB specimens were manually healed and retested using the same methodology. Healing was achieved by manual injection with the mixture containing 75 wt% EPON 828—25 wt% ethyl phenylacetate and 3.25 phr of solid state scandium (III) triflate. A typical load displacement curve illustrating pristine fracture behaviour and crack arrest is presented in figure 3(a). The average healing efficiency calculated from the difference of maximum peak loads ($P_{max}$) is 52.5%. This low value is associated with the lack of non-repairable fibre bridging developed in pristine specimens. Figure 4 illustrates fracture surfaces of DCB specimens after the initial tests and after the manual repair. A cohesive debonding mode of injected and polymerised epoxy resin is observed which suggests that the strength of the interface between carbon fibres and the epoxy resin is higher than fracture strength of the resin. Detailed data for healing efficiency (η) and initial interlaminar fracture toughness ($G_{IC}$) are summarised in table 2.

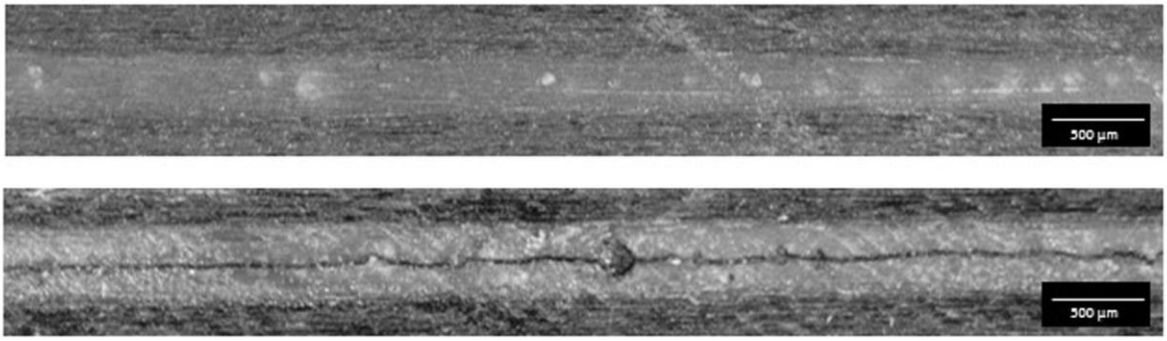


Figure 5. Artificially created resin-pocket in representative DCB specimens (a) before and (b) after the initial mode I fracture toughness test.

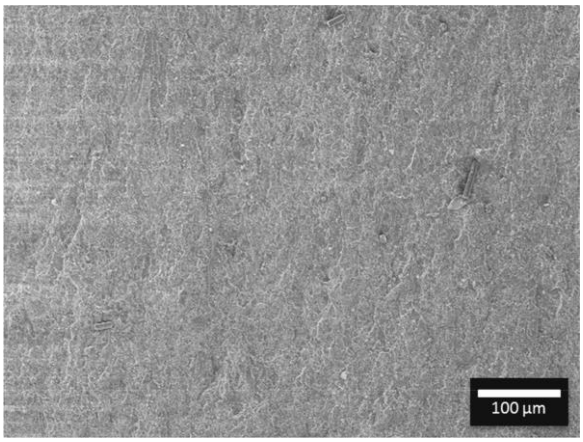


Figure 6. SEM image of DCB fracture surfaces of a specimen containing resin pocket and no microcapsules and catalyst dispersed in the damage region.

The data collected here indicate that the resin formulation described in the literature [36, 37] is capable of successful restoration of mode I properties of the selected epoxy resin/ carbon fibre material (SE70, Gurit, UK). In liquid phase, the healing agent has a low viscosity and long gel time allowing penetration and wetting of the fractured surfaces. In the solidified state, the epoxy resin is plasticised by the organic solvent (EPA) what results in increased fracture toughness that in non-modified resin. Such modification results in steady and progressive crack propagation for the manually healed DCB specimens as presented in figure 3(a).

### 3.3. Autonomous self-healing

Autonomous self-healing was determined for a series of specimens containing microcapsules and catalyst in the interleave region (figure 5). First, tests were performed for maximum load of microcapsules (26 wt%) and load of cata-lyst adapted from literature (2.5 wt%) [9]. Figure 3(b) repre-sents a typical load–displacement curve for virgin and healed DCB specimens. The observed crack arrest indicates that the chemistries embedded in the interleave region are active after composite manufacturing and polymerised healing agent bonds the fractured surfaces. However, the average self-healing efficiency is not exceeded 10% of the value of maximum load at the crack onset. Embedded healing chemistries caused substantial decrease in initial maximum load ($P_{max}$) at crack onset and corresponding $G_{IC}$ values (table 2). It indicates that microcapsules and catalyst have a detrimental effect on the proposed FRP composite. Figure 6 shows a representative fracture surface for Control 2 speci-men revealing no features of crack arrest in the SA 70 epoxy resin. Surface morphology for autonomous specimens (figure 7) illustrates ruptured microcapsules, catalyst particles and thin film created by polymerised epoxy healing agent covering the fracture surface. The excessive porosity created by liquid filled microcapsules was assumed to be responsible for such high decrease in materials virgin properties. Further work focused on optimisation of microcapsules size and catalyst load with the aim of increasing the self-healing rate and examining the effect of healing components on material performance.

3.3.1. The effect of microcapsules load. Self-healing was determined for specimens containing variable concentrations of microcapsules dispersed in the composite interleave (table 1). It was assumed that the low healing efficiency is associated with low bonding area in the proof of the concept study (see entry ‘autonomous’ in table 2). Loading of microcapsules was calculated according to the mass of SA 70 resin used in the manufacturing of each separate panel and corresponds to 5.5, 11 and 26 wt%. Here, the diameter of microcapsules was limited to 250–420 µm in order to ensure their full rupture by a propagating crack and to decrease the induced porosity. Fracture morphology illustrating microcapsule distribution in the damage zone is presented in figure 8. Table 2 summarises results, which indicate that recovery of mode I is independent of microcapsule loading. Moreover, an average 12% self-healing was observed for all test specimens. It indicates that volume of encapsulated liquid monomer is enough to cover the fracture surface and bridge them after polymerisation. It was assumed that the low self-healing rate is a result of low crosslinking density in the newly formed epoxy resin. Increasing the number of polymerisation centres could result in tougher polymer that should bond the fractured surfaces more effectively. Additionally, a minimum decrease in initial fracture toughness ($G_{IC}$) was observed between specimens without microcapsules (Control 2) and containing 11 wt% of microcapsules (250–420 µm). Reducing the number of

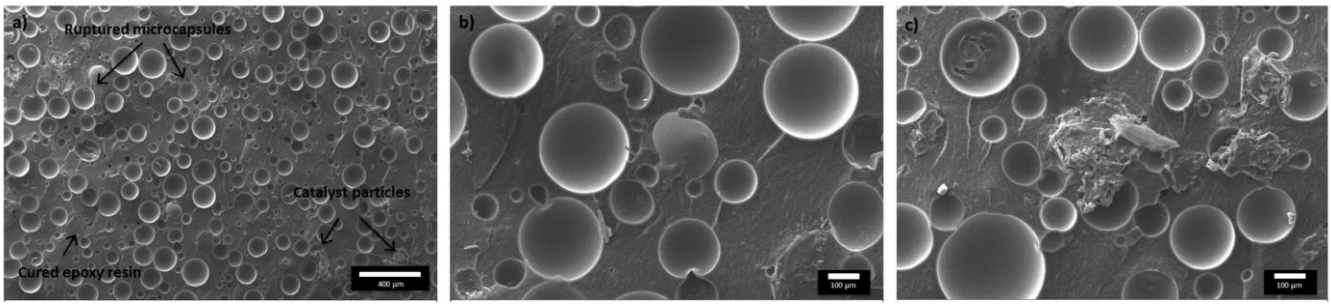


Figure 7. (a) Fracture morphology of a specimen containing 25 wt% microcapsules dispersed in polymeric matrix and 2.5 wt% of catalyst particles, (b) image illustrating ruptured microcapsules at higher magnification and (c) image illustrating undissolved catalyst particles covered in thin film of epoxy healing agent.

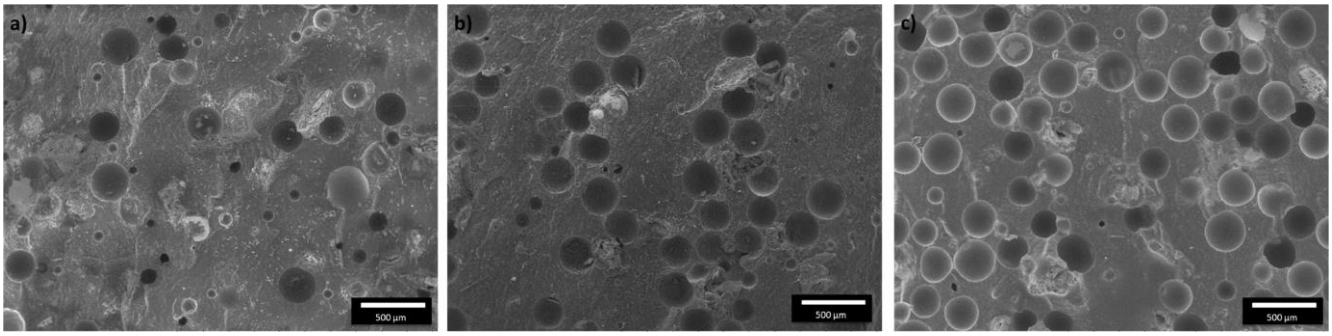


Figure 8. SEM images of surface morphologies for DCB specimens containing variable loading of microcapsules embedded in the interleave region; (a) 5.5 wt%, (b) 11 wt% and (c) 26 wt%; at constant load of catalyst (2.5 wt%).

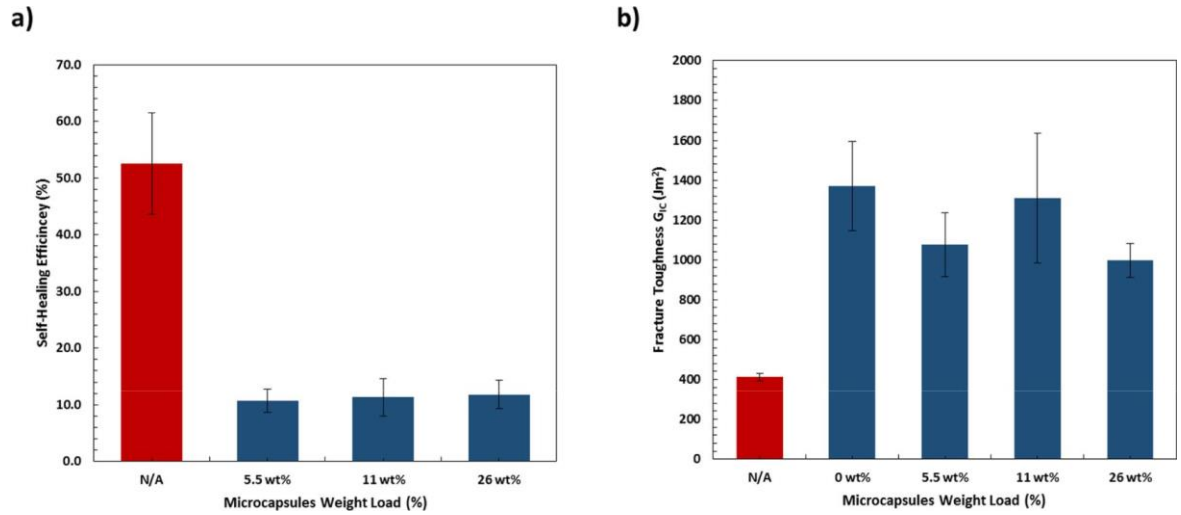


Figure 9. (a) Self-healing efficiency and (b) initial fracture toughness ($G_{IC}$) for specimens containing variable volume of self-healing phase using microcapsules within 250–450 µm range.

microcapsules in the damage zone, an increase of the maximum peak load ($P_{max}$) and calculated fracture toughness ($G_{IC}$) is observed (table 2). Reducing the number of the stress concentration regions, a 16 N increase of $P_{max}$ and 251 J $m^{-2}$ of $G_{IC}$ is calculated bringing the value close to Control 2 specimen. These facts suggest that the size and size distribution of microcapsules can be tailored in FRP composites to deliver healing functionality with minimum detrimental effect. In further work, DCB specimens were prepared at this microcapsules concentration, the work aimed to increase the self-healing rate by manipulating the catalyst concentration in the system.

3.3.2. The effect of $Sc(OTf)_3$ concentration. To increase the self-healing rate and to understand the effect of catalyst particles on initial fracture properties, a series of specimens containing variable loadings of $Sc(OTf)_3$ at constant concentration of microcapsules (11 wt%) were prepared and tested. Specimens were healed for 48 h in order to ensure full crosslinking of released healing agent. Table 3 summarises

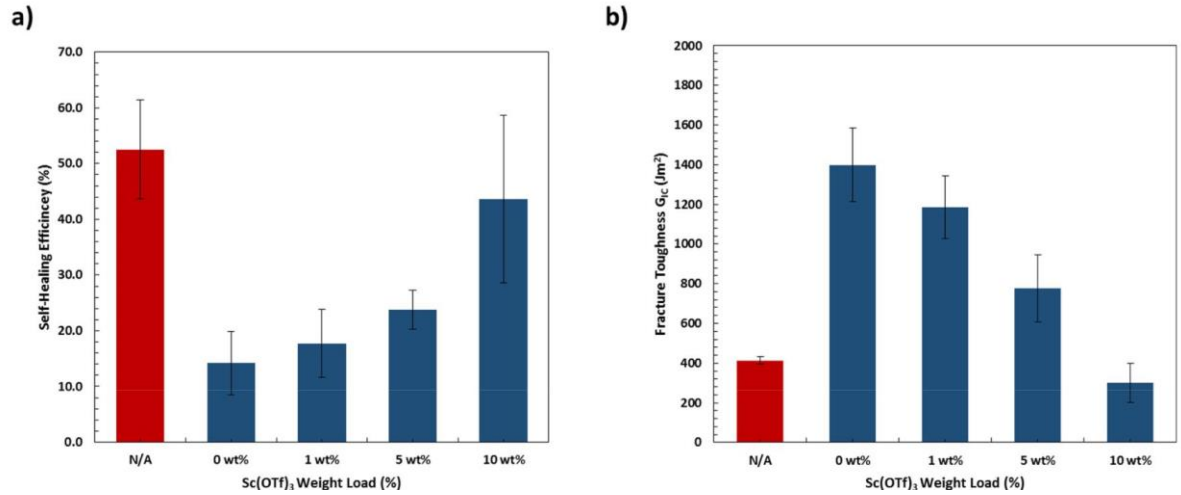


Figure 10. (a) Self-healing efficiency and (b) initial fracture toughness ($G_{IC}$) for specimens containing variable weight of $Sc(OTf)_3$ at 11 wt% microcapsules (250–450 μm range).

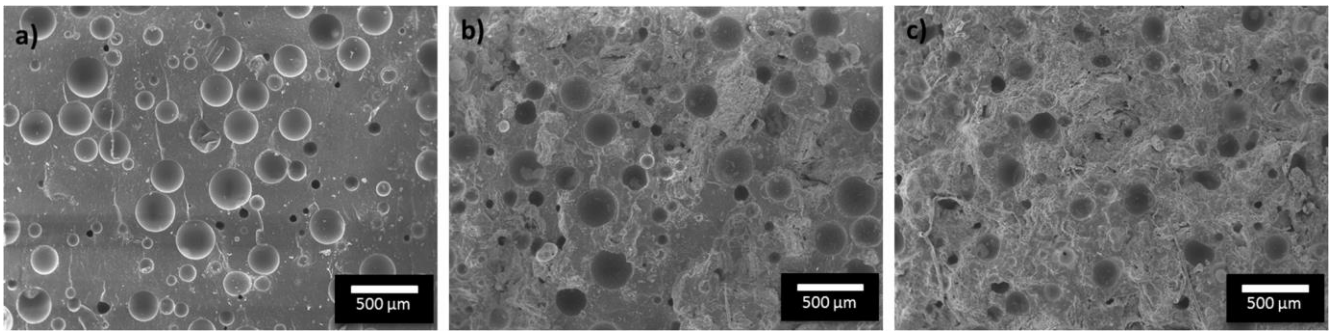


Figure 11. Fracture morphologies of DCB samples containing 11 wt% of capsules and (a) 1 wt% catalyst, (b) 5 wt% catalyst and 10 wt% catalyst.

Table 3. Summary of healing efficiency (η) and fracture toughness ($G_{IC}$) in dependence on $Sc(OTf)_3$ load dispersed in the interleave region.

| Designation | Vol % | Capsules size (μm) | Initial load $P_{Virgin}$ (N) | Healed load $P_{Healed}$ (N) | η (%) | Initial $G_{IC}$ (J m$^{-2}$) | Healing temp |
|---|---|---|---|---|---|---|---|
| Control 2 | — | — | 81.0 ± 6.4 | — | — | 1371 ± 224 | |
| 11 wt_0.0 wt% | 10 | 250–420 | 83.1 ± 5.3 | 13.2 ± 1.3 | 14.2 ± 5.7 | 1399 ± 186 | |
| 11 wt_1.0 wt% | 10 | 250–420 | 73.4 ± 9.5 | 12.7 ± 3.2 | 17.7 ± 6.1 | 1184 ± 158 | 80 °C |
| 11 wt_5.0 wt% | 10 | 250–420 | 59.4 ± 6.9 | 14.0 ± 0.5 | 23.8 ± 3.5 | 777 ± 170 | |
| 11 wt_10 wt% | 10 | 250–420 | 38.4 ± 7.8 | 15.8 ± 2.0 | 43.6 ± 15.0 | 301 ± 99 | |

the test results where figure 10 presents a series of results collected for the specimens containing 0, 1, 5 and 10 wt% of $Sc(OTf)_3$. The maximum 44% of self-healing was obtained at maximum catalyst loading (10 wt%) and decreases with lower load of the catalyst. In addition, an average of 14% recovery was obtained for specimens containing no catalyst particles, indicating the presence of solvent promoted self-healing [15]. It is concluded that the increase of healing rate is associated with a substantial decrease in initial fracture properties. Results in table 3 suggest that the initial fracture toughness ($G_{IC}$) decreased to 301 J m$^{-2}$, which is close to that observed for Control 1 specimens containing no resin interleave— 413 J m$^{-2}$ (table 2). The values of the maximum peak load ($P_{max}$) for all healed specimens remains in the same range (13.2–16.0 N) indicating that the presence of catalyst has no beneficial effect on the mode I recovery. Figure 11 illustrates altered fracture surfaces containing 1, 5 and 10 wt% of the catalyst particles. The fracture morphology containing only microcapsules is illustrated in figure 12.

## 4. Discussion

An autonomous self-healing based on epoxy resin filled microcapsules and solid phase catalyst is demonstrated in a high performance CFRP composite (cured at 100 °C for 100 min) and examined for its performance. The crack arrests observed on the load–displacement curves (figure 2) indicate

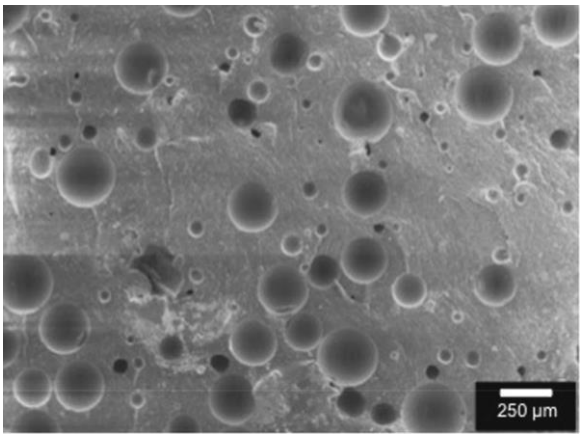


Figure 12. SEM image of DCB specimen containing 11 wt% of microcapsules (250–450 µm range) in the damage region.

that the released epoxy resin undergoes polymerisation after contact with dispersed catalyst particles and bonds the frac-ture surfaces. The SEM analysis (figure 7) revealed ruptured microcapsules, residual catalyst particles and thin film of epoxy healing agent covering the fracture surfaces. It was found that mode I recovery is dependent on the catalyst loading and reached 44% maximum (comparable to 52% for manually healed). However, this increase is associated with substantial (3×) decrease in initial fracture toughness ($G_{IC}$) and the maximum load at the crack onset ($P_{max}$). Never-theless, it is demonstrated that concentration of microcapsules embedded in the damage region can be tailored to achieve self-healing with minimal detrimental effect on the structure. Moreover, reducing the number of microcapsules by remov-ing the samples with size smaller than 250 µm, an increase in maximum peak load ($P_{max}$) and fracture toughness ($G_{IC}$) is observed. It suggest that the wide range of microcapsules' diameter generates excessive porosity that impedes the properties of the host material. Low healing efficiency was associated with low cross-linking rate initiated by the chosen catalytic curing agent ($Sc(OTf)_3$) and its presence as a solid. Attempts to increase the self-healing rate by tailoring the catalyst loading resulted in further decrease of the composite fracture properties without any gain of mode I recovery.

While the concentration of microcapsules has no effect on self-healing efficiency (table 2), their higher concentration caused a decrease in the host material's initial fracture toughness and change in fracture morphology. This trend was already observed in epoxy based polymers [9, 10, 22], adhesives [40] and woven composites [5, 12, 19, 23], where inclusion of microcapsules always gave rise to a decrease in material attributes. Microcapsules and catalyst particles are considered as voids, creating discontinuities in the host polymer and acting as stress concentrations. To minimise the effect, microcapsule diameter was restricted to 250–420 µm which resulted in average $G_{IC}$ close to virgin at 11 wt% of microcapsules (figure 9). In addition, inclusion of the inter-leave region filled with capsules resulted in a 3× increase in $G_{1c}$ when compared to blank specimens (table 2). It is asso-ciated with the presence of bulk epoxy resin at the crack initiation point. In blank specimens the crack is initiated at the weak interface between the carbon fibre and the polymeric matrix. In the developed structure, the crack is initiated in a bulk epoxy resin (SA 70) that exhibited much higher fracture toughness than the strength of the interface.

To increase the self-healing efficiency, a series of spe-cimens containing higher concentrations of solid phase cata-lyst were prepared and tested. While the healing efficiency increased with catalyst concentration, a substantial reduction in initial fracture toughness was recorded (figure 10). The maximum healing efficiency (44%) reached values for control specimens repaired by manual injection (52%). Similarly, observed reduction of fracture properties is associated with excessive presence of voids created by scandium (III) triflate particles in the fracture planes. It is illustrated in figures 11(b) and (c) where microcapsules are surrounded by $Sc(OTf)_3$ particles that significantly alter the fracture morphology. In general, undissolved catalyst particles, their detrimental effect on material attributes, and little beneficial effect on healing rate, suggest that application of a microcapsule—solid phase catalyst system in high performance FRP composite struc-tures is questionable.

In summary, an autonomous self-healing is demonstrated and assessed for its performance in a unidirectional FRP composite structure. The work shows that microcapsule healing can be adapted and optimised in unidirectional FRP composite materials. However, the investigated system, which relies on a distribution of microcapsules and a solid phase catalyst, is detrimental to the FRP composite. Inter-laminar fracture toughness ($G_{IC}$) is severely affected by pre-sence of both healing components. The low solubility of scandium (III) triflate in liquid resin, it is premature con-sumption, the detrimental effect on the host structure and little beneficial effect on healing efficiency were identified as substantial limitations for commercialisation. Therefore, an alternative system based on a single component healing sys-tem or integrated double capsules should be considered for such an application. A microcapsule—catalyst system could be considered as an adhesive, where inhibited reactivity is required for extended period of time. Nevertheless, it has been demonstrated that microcapsule self-healing can be achieved in a unidirectional FRP composite cured at high temperature (100 °C) and located in regions of possible damages.

## 5. Conclusions

An autonomous self-healing system was demonstrated in a high performance unidirectional FRP composite using epoxy resin filled microcapsules and a solid phase catalyst ($Sc(OTf)_3$). Healing efficiency and effect of microcapsules on the structure was assessed using mode I fracture toughness test-ing. A maximum of 52% and 44% recovery was obtained for specimens healed manually and autonomously, respectively. However, inclusion of resin interleaves and healing chemis-tries in laminates have a detrimental effect on their perfor-mance. It has been demonstrated that amount of both healing

components can be tailored to avoid a decrease in material performance.

Furthermore, the application of a solid phase catalyst remained questionable due to its low efficiency in the polymerisation of encapsulated epoxy healing agent. A similar crack arrest rate after healing was obtained for specimens containing only microcapsules (12%). Nevertheless, autonomous self-healing was achieved in a structural component based on commercial epoxy resin/carbon fibre tape (SE70 Carbon, Gurit, UK). It is also demonstrated that the healing chemistry can be located in regions of possible damage in composite components.

## Acknowledgments

The authors would like to acknowledge the European Union Seventh Framework Programme for supporting this research under FP7-MC-ITN-290308 'SHeMat—Training Network for Self-Healing Materials from Concept to Market'.

## References

[1] Zhang S and Zhao D (ed) 2012 Processing science for polymeric composites in aerospace Aerospace Materials Handbook (Boca Raton: CRC Press) p 461–92

[2] Binder W H 2013 Self-Healing Polymers (Germany: Wiley-VCH)

[3] Blaiszik B J, Kramer S L B, Olugebefola S C, Moore J S, Sottos N R and White S R 2010 Self-healing polymers and composites Annu. Rev. Mater. Res. 40 179–211

[4] Hager M D, Greil P, Leyens C, van der Zwaag S and Schubert U S 2010 Self-healing materials Adv. Mater. 22 5424–30

[5] Kessler M and White S 2001 Self-activated healing of delamination damage in woven composites Composites A 32 683–99

[6] Wilson G O, Caruso M M, Reimer N T, White S R, Sottos N R and Moore J S 2008 Evaluation of ruthenium catalysts for ring-opening metathesis polymerization-based self-healing applications Chem. Mater. 20 3288–97

[7] Wilson G O, Porter K A, Weissman H, White S R, Sottos N R and Moore J S 2009 Stability of second generation Grubbs' alkylidenes to primary amines: formation of novel ruthenium–amine complexes Adv. Synth. Catal. 351 1817–25

[8] Kamphaus J M, Rule J D, Moore J S, Sottos N R and White Sr 2008 A new self-healing epoxy with tungsten (VI) chloride catalyst J. R. Soc. Interface 5 95–103

[9] Coope T S, Mayer U F J, Wass D F, Trask R S and Bond I P 2011 Self-healing of an epoxy resin using scandium(III) triflate as a catalytic curing agent Adv. Funct. Mater. 21 4624–31

[10] Xiao D S, Yuan Y C, Rong M Z and Zhang M Q 2009 Self-healing epoxy based on cationic chain polymerization Polymer 50 2967–75

[11] Yuan Y C, Rong M Z, Zhang M Q, Chen J, Yang G C and Li X M 2008 Self-healing polymeric materials using epoxy/mercaptan as the healant Macromolecules 41 5197–202

[12] Yuan Y C et al 2011 Self-healing of low-velocity impact damage in glass fabric/epoxy composites using an epoxy–mercaptan healing agent Smart Mater. Struct. 20 015024

[13] Jin H, Mangun C L, Stradley D S, Moore J S, Sottos N R and White SR 2012 Self-healing thermoset using encapsulated epoxy-amine healing chemistry Polymer 53 581–7

[14] McIlroy D A, Blaiszik B J, Caruso M M, White S R, Moore J S and Sottos N R 2010 Microencapsulation of a reactive liquid-phase amine for self-healing epoxy composites Macromolecules 43 1855–9

[15] Caruso M M, Blaiszik B J, White S R, Sottos N R and Moore J S 2008 Full recovery of fracture toughness using a nontoxic solvent-based self-healing system Adv. Funct. Mater. 18 1898–904

[16] Caruso M M, Delafuente D A, Ho V, Sottos N R, Moore J S and White S R 2007 Solvent-promoted self-healing epoxy materials Macromolecules 40 8830–2

[17] Kirkby E L, Rule J D, Michaud V J, Sottos N R, White S R and Månson J-A E 2008 Embedded shape-memory alloy wires for improved performance of self-healing polymers Adv. Funct. Mater. 18 2253–60

[18] Kirkby E L, Michaud V J, Månson J-A E, Sottos N R and White S R 2009 Performance of self-healing epoxy with microencapsulated healing agent and shape memory alloy wires Polymer 50 5533–8

[19] Yin T, Zhou L, Rong M Z and Zhang M Q 2008 Self-healing woven glass fabric/epoxy composites with the healant consisting of micro-encapsulated epoxy and latent curing agent Smart Mater. Struct. 17 015019

[20] Xiao D S, Yuan Y C, Rong M Z and Zhang M Q 2009 A facile strategy for preparing self-healing polymer composites by incorporation of cationic catalyst-loaded vegetable fibers Adv. Funct. Mater. 19 2289–96

[21] Blaiszik B J, Caruso M M, McIlroy D A, Moore J S, White S R and Sottos N R 2009 Microcapsules filled with reactive solutions for self-healing materials Polymer 50 990–7

[22] Brown E N, White S R and Sottos N R 2004 Microcapsule induced toughening in a self-healing polymer composite J. Mater. Sci. 39 1703–10

[23] Arnold U, Habicht W and Döring M 2006 Metal-doped epoxy resins—new catalysts for the epoxidation of alkenes with high long-term activities Adv. Synth. Catal. 348 142–50

[24] Trask R S, Williams G J and Bond I P 2007 Bioinspired self-healing of advanced composite structures using hollow glass fibres J. R. Soc. Interface 4 363–71

[25] Williams G, Trask R and Bond I 2007 A self-healing carbon fibre reinforced polymer for aerospace applications Composites A 38 1525–32

[26] Pang J W C and Bond I P 2005 'Bleeding composites'—damage detection and self-repair using a biomimetic approach Composites A 36 183–8

[27] Toohey K S, Sottos N R, Lewis J A, Moore J S and White SR 2007 Self-healing materials with microvascular networks Nat. Mater. 6 581–5

[28] Hamilton A R, Sottos N R and White S R 2012 Pressurized vascular systems for self-healing materials J. R. Soc. Interface 9 1020–8

[29] Chen X et al 2002 A thermally re-mendable cross-linked polymeric material Science 295 1698–702

[30] Hong K and Park S 1999 Preparation of polyurea microcapsules with different composition ratios: structures and thermal properties Mater. Sci. Eng. A 272 418–21

[31] Kalista S J, Ward T C and Oyetunji Z 2007 Self-healing of poly(ethylene-co-methacrylic acid) copolymers following projectile puncture Mech. Adv. Mater. Struct. 14 391–7

[32] Varley R J and Parn G P 2012 Thermally activated healing in a mendable resin using a non woven EMAA fabric Compos. Sci. Technol. 72 453–60

[33] Cordier P, Tournilhac F, Soulié-Ziakovic C and Leibler L 2008 Self-healing and thermoreversible rubber from supramolecular assembly Nature 451 977–80

[34] Peterson A M, Kotthapalli H, Rahmathullah M A M and Palmese G R 2012 Investigation of interpenetrating polymer networks for self-healing applications Compos. Sci. Technol. 72 330–6

[35] Feng J, Xiong L, Wang S, Li S, Li Y and Yang G 2013 Fluorescent temperature sensing using triarylboron compounds and microcapsules for detection of a wide temperature range on the micro- and macroscale Adv. Funct. Mater. 23 340–5

[36] Coope T S, Wass D F, Trask R S and Bond I P 2013 Metal triflates as catalytic curing agents in self-healing fibre reinforced polymer composite materials Macromol. Mater. Eng. n/a–n/a available from (http://doi.wiley.com/10.1002/mame.201300026)

[37] Coope T S, Wass D F, Trask R S and Bond I P 2014 Repeated self-healing of microvascular carbon fibre reinforced polymer composites Smart Mater. Struct. 23 115002

[38] ASTM D5528-01 Standard test method for mode I interlaminar fracture toughness of unidirectional fiber-reinforced polymer matrix composites www.astm.org

[39] Bolimowski P A, Bond I P and Wass D F 2016 Robust synthesis of epoxy resin-filled microcapsules for application to self-healing materials Phil. Trans. R. Soc. A 374 20150083

[40] Jin H et al 2013 Fracture behavior of a self-healing, toughened epoxy adhesive Int. J. Adhes. Adhes. 44 157–65